



Photocatalytic degradation of MB by TiO₂: studies on recycle and reuse of photocatalyst and treated water for seed germination

Kumari Sonu¹ · Shivaraju Harikaranahalli Puttaiah¹ · Vikram Srinivasa Raghavan² · Sai Siva Gorthi²

Received: 30 June 2020 / Accepted: 6 April 2021 / Published online: 29 April 2021

© The Author(s), under exclusive licence to Springer-Verlag GmbH Germany, part of Springer Nature 2021

Abstract

Photocatalysis is an effective way for treatment of wastewater and degradation of dyes. It is important to assess the reusability of photocatalyst and treated water after the treatment process. In this study, the photocatalytic activity of TiO₂ (titanium dioxide) and TiO₂-TMAOH (titanium dioxide-tetramethylammonium hydroxide) was analyzed for degradation of methylene blue dye. Enhanced degradation of methylene blue is observed while treated with TiO₂-TMAOH with photodegradation efficiency (PDE) 80% within 20 min. A further study shows the reusability of TiO₂ for degradation of dye for six cycles with a decrease in photodegradation efficiency from 90% (cycle-1) to 50% (cycle-2). Fourier transform infrared spectroscopy (FTIR), energy-dispersive X-ray spectroscopy (EDX), and cyclic voltammetry (CV) analysis were carried out to identify the functional groups in treated water, traces of titanium, and TMAOH, respectively. Seed germination of *Vigna radiata* using TiO₂- and TiO₂-TMAOH-treated water shows equivalent and consistent growth. Water quality analysis of treated water shows improved biochemical oxygen demand (BOD) level (1.5 mg L⁻¹), which is suitable for reusability of water for many applications. The outcomes suggest treated water can be used for irrigation and plantation purposes.

Keywords Photocatalysis · Nanomaterials · Dye degradation · Elemental analysis · Recycled water · Seed germination

Introduction

Advanced oxidation process has gained the attention of scientists and researchers in recent years as it is proved to be one of the most promising methods for the degradation of most of the pollutants in wastewater effluents (Khataee et al. 2009). Nanomaterials of ZnO, SnO₂, and TiO₂ are widely used for treatment purposes (Neppolian et al. 2002a, 2002b). TiO₂ nanostructures are well-established materials for photocatalytic dye degradation due to their photo-catalytically stable nature, ease of production at low cost, and less risk to environment (Akpan and Hameed 2009; Gupta et al. 2006; Styli

di et al. 2004; Natarajan et al. 2011). Light source and catalysts are two important factors during heterogeneous photocatalysis (Styliidi et al. 2003). TiO₂-Based photocatalysis involves irradiation of UV light to enhance the degradation process. When UV rays fall on TiO₂, the e⁻/h⁺ present in the conduction band and valence band moves towards the oxide surface and reacts with chemically adsorbed O₂/OH⁻/H₂O molecules. This mechanism produces the reactive O₂⁻ (superoxide ions) and OH radicals species during the photocatalysis process, which reacts with the functional groups present in dyes and other organic pollutants (Chen et al. 2015; Zhao et al. 1998; Styliidi et al. 2003). Methylene blue is an organic dye and soluble in water; this gets in contact and absorbed by wet soil during discharge. Phototransformation of methylene blue in water with solar irradiation shows dissipation half-life (DT50) of 17.2 days, 95% of degradation when present in biodegraded water for 20 days, 91% of degradation when present in water for 15 days, 88% for 10 days, and 76% for 5 days showing that it can be easily degraded. TiO₂ is used with other nanomaterials and is also doped with metals to treat several effluents and particularly dye-based contaminants. Doping of transition metals, earth metals, and non-metals is performed to improve the performance by enhancing the

Responsible Editor: Sami Rtimi

✉ Kumari Sonu
sonims2325@gmail.com

¹ Division of Environmental Science, Department of Water and Health, JSS Academy of Higher Education and Research, Mysore, Karnataka 570015, India

² Optics and Microfluidics Instrumentation Lab, Department of Instrumentation and Applied Physics, Indian Institute of Science, Bengaluru, Karnataka 560012, India

redox potential (Teh and Mohamed 2011). Other metal oxides such as ZnO, SiO₂, Al₂O₃, and ZrO₂ are used along with TiO₂ to enhance the photocatalytic activity (Comparelli et al. 2005).

TiO₂ is an excellent photocatalyst but can get activated only at 387 nm UV wavelength due to its bandgap of 3.2 eV, which is less than 8% of the sunlight. When optimal UV light falls on the catalyst surface, it agitates the electron present in the valence band leaving behind a positive hole, moving towards conduction band (Salehi et al. 2012). Impregnation of e⁻ produces oxidizing species such as O₂⁻, OH[•] radicals by reducing the surface chemisorbed oxidants which later leads to the photodegradation of dye (Stylidi et al. 2003). Trapping of electrons is prevented by the presence of oxygen which reduces to form superoxide ionic radicals in the conduction band. The reaction between the h⁺ and the adsorbed water molecules leads to the formation of OH radicals (Diaz-Urbe et al. 2014; Kim and Lee 2003; Vallejo et al. 2015).

Increasing the OH radical on the catalyst surface enhances active sites for photodegradation. OH groups present on TiO₂ surface improve photocatalytic activity at high concentration (Wu et al. 2017; Zhang et al. 2017). Feizi et al. 2012. reported the impact of nano and bulk TiO₂ on germination of seed, but uptake and bioaccumulation of particles have not been verified.

Dye present in the wastewater discharge is absorbed by the plants during transpiration. During this process, along with water, other chemicals present in the soil also get absorbed by the plants. Further, these chemicals translocate and get accumulated in different parts of the plants. translocate and get accumulated in the different parts of the plants. The water gets evaporated from the parts of the plants, but the absorbed dyes remain in the system. During continuous absorption and evaporation of water, the chemicals and dyes are absorbed and accumulated into the plant system. Growth of plants is affected after reaching the threshold limit of dye absorption. Furthermore, it leads to bioaccumulation if consumed by humans and animals. Treated wastewater can be reused for irrigation purposes, and it is important to remove traces of heavy metals and dyes before using it for irrigation and plantation. These contaminants even prevent micro- and macronutrients absorbed by the crops and plants from the soil. The contaminants decrease the fertility of the soil after prolonged exposure and get absorbed repeatedly by the crops and plants leading to food chain and consumption. It is important to validate traces of contaminants and transpiration of treated water to determine the fate of plants and seeds after absorption of treated wastewater.

In this work, TMAOH as a surfactant prevents particle aggregation (Andrade et al. 2012). With the combination of TMAOH with a good source of OH⁻ group, the photodegradation property of TiO₂ can be enhanced. By tuning the concentration of TMAOH, it is possible to control the photocurrent response of TiO₂ structures under UV

illumination (Dong et al. 2010; Rodriguez et al. 2017; Chen et al. 2015). Hydroxyl radical on the surface of TiO₂ is important to reduce the particle aggregation and increase of these radical initiates deformation for the structures of TiO₂ (Wu et al. 2017). Since TiO₂ is the most preferred and explored material for photocatalytic degradation of dye, it is important to analyze the reusability of the material to treat dye samples and to study the degradation efficiency of TiO₂ during multiple usages. To explore this focus, we have used two types of TiO₂ nanostructures ((a) TiO₂ and (b) TiO₂-TMAOH) to analyze the degradation of methylene blue dye under low-power UV irradiation. Furthermore, the treated water is analyzed for the seed germination process; this process is undertaken to demonstrate the reusability of the treated water for the seed germination process.

Materials and methods

Titanium isopropoxide 98% purity (TTIP) and tetramethylammonium hydroxide (TMAOH) are purchased from Spectrochem Pvt. Ltd., Mumbai, India. Acetic acid 99–100% (Merck specialization private limited) and methylene blue powder (SDFCL SD Fine-Chem Limited) are utilized for preparing stock solution for performing further experiments.

TiO₂ nanopowders were synthesized by hydrothermal process. Eight milliliters of TTIP is added to 17 ml of distilled water (DI). Acetic acid (37%) is added dropwise to the solution to maintain the pH around 1.5 resulting in the formation of white precipitate. The solution was stirred for 30 min at room temperature in a Teflon container. The Teflon-lined autoclave is maintained at 160 °C in a hot air oven for 12 h and allowed to reach room temperature. The supernatant is removed, and DI water is added to the precipitate for the centrifugation process at 1500 rpm for 5 min. After this process, the precipitate is washed to attain neutral pH. The precipitate is heated at 60 °C in the hot air oven. The end-product is characterized and used for experiments without any further purification.

For the preparation of TiO₂-TMAOH, 50 µl of TMAOH (0.5 % v/v) was added to 0.02 g of TiO₂ powder and sonicated for 15 min. Six parts per million of methylene blue (MB) is prepared, and the concentration is maintained for all experiments. Ten milliliters of 6 ppm MB is used to analyze the photocatalytic activity of TiO₂ nanoparticles. The experiments were performed using UV light source 8 W (365 nm), and actual power irradiated at the sample is 2 mW cm⁻².

Experimentation

The photocatalytic efficiency of TiO₂ nanoparticles is analyzed in two categories: (a) TiO₂ nanoparticles and (b) TiO₂-

OH, treated with TMAOH, which are dispersed separately in two vials consisting 10 ml (6 ppm) MB aqueous solution. This is further placed in a UV chamber for irradiation. UV-Vis measurements were recorded at each interval (20, 40, 60, 120, 180, 240, and 300 min). During each interval, 1 ml of the sample is carefully taken from the 10-ml vial for UV-Vis analysis. After the analysis, the sample was re-dispersed with forward pipetting in the corresponding vials. The treated samples are subjected to further analysis using FTIR, EDX, UV-Vis, pH, and zeta techniques. After this process, the treated samples are used to analyze the seed germination process using *Vigna radiata* seeds without any further purification. Seed germination analysis is conducted by dispersing 1 ml quantity of treated water into 10-ml glass vials with *Vigna radiata* seeds. The germination process is observed for 1 week, and no further treated water is added to the vials during this period. Standard scaling measurement is followed to analyze the growth profile of different samples.

Results and discussion

Photodegradation efficiency is calculated for samples using (a) TiO_2 and (b) TiO_2 -TMAOH; the results are shown in Fig. 1. The plots reveal that samples treated with TiO_2 enhance adsorption and induce coagulation and sedimentation of dye substance, whereas TiO_2 -TMAOH enhances the dye degradation process. In the present study, TMAOH has been used as surfactant which prevents aggregation and precipitation of TiO_2 nanoparticles and enhances the photocatalytic activity by producing more OH^- as it reacts in the solution to form TMA and OH^- (Chen et al. 2007). In both cases, the

treated samples are analyzed to identify trace elements and compounds.

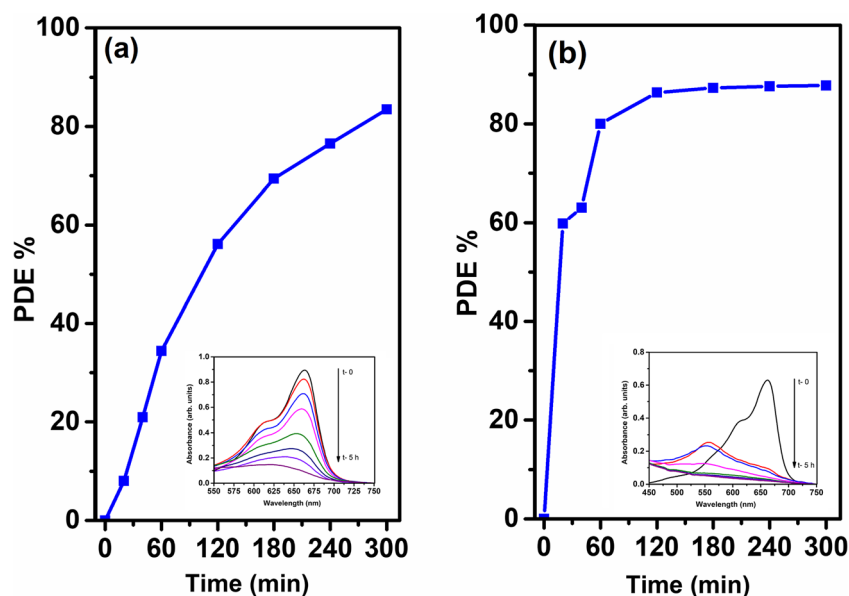
Reusability of sediment substance with TiO_2 is also explored for a few cycles with the same concentration of dye. During this analysis, the treated supernatant was carefully removed from the sample and a new untreated sample with the same dye concentration was added. This process is analyzed specifically to check the effectiveness of TiO_2 particles sediment along with treated dye substance. All the samples were mixed at a particular time interval to enable proper mixing of sedimented substances with new samples.

Zeta potential values were recorded for dispersed TiO_2 nanoparticles in the water at the 1-h interval for 5 h. The average hydrodynamic diameter is 178 nm, and zeta potential is 40 mV; this confirms that the particles exhibit good stability for the duration of the experiment.

Photocatalytic activity of TiO_2 and TiO_2 -OH

Photocatalytic profiles of both TiO_2 and TiO_2 -OH are shown in Fig. 1a and b. The plots show the photodegradation efficiency (PDE) of both systems, and the inset image shows the absorbance trend of samples recorded for 5 h (i.e., 300 min). In both cases, the photocatalytic activity is observed as more than 80% for the mentioned duration. The concentration of TiO_2 catalyst present in the MB samples is 1%. At this concentration, the photocatalyst shows significant performance in the MB treatment process. Compared to TiO_2 , the TiO_2 -OH shows rapid activity before 60 min. This mechanism is due to the increased availability of OH^- radicals present on TiO_2 systems, which leads to a rapid reaction with MB structure (Dong et al. 2010; Rodriguez et al. 2017; Chen et al. 2015).

Fig. 1 PDE% of MB using **a** TiO_2 and **b** TiO_2 -OH. Inset images show UV absorption spectra



Increased OH radicals due to addition of TMAOH into the solution are responsible for uniform dissociation of the TiO₂ photocatalyst during the reaction (Wu et al. 2017). The conventional approach of photocatalytic dye treatment involves two categories such as dye degradation in sample and dye removal from the sample through coagulation and flocculation processes that can be attributed to physicochemical adsorption. In this work, both techniques are implemented to analyze the photodegradation rate, efficiency, and reusability of the treated water. The inset image in Fig. 1a shows the usual mechanism of the reaction of TiO₂ photocatalyst with MB dye, and the trend in absorbance shows progress in the degradation of MB. The absorbance plot in Fig. 1b inset shows the treatment of MB using TiO₂-OH catalyst; a blue shift in the spectra is observed that represents the phase transformation of the catalyst. This principle is a function of charge density with the photocatalyst compound that leads to determining dimer or trimer complex (Smirnova et al. 2019; Yuan et al. 2019).

Figure 2a–f show the images of MB before and after the treatment process. The images show the degradation process of MB in both cases for 300-min duration. Sedimentation of substance is visible in Fig. 2c; the TiO₂ catalyst reacts with MB dye under UV irradiation and initiates the coagulation process. This process further leads to sedimentation of the treated substance. In this case, the supernatant is considered

the treated water and carefully separated from the sedimented substance. In another scenario, the active –OH functional on TiO₂ undergoes a similar treatment process but at a faster rate compared to reaction using bare TiO₂ nanoparticles. This process is shown in Fig. 2e; in this case, clear and transparent liquid is observed with no sedimentation compared to the previous case as shown in Fig. 2c. Furthermore, the treated samples are analyzed using FTIR and EDX techniques to determine the functional groups and trace elements corresponding to the samples. Before validating the traces present in the treated samples using bare TiO₂ catalyst, the sedimented substance is carefully isolated from the supernatant and subjected to react with new MB samples. This process is carried out to investigate the reusable limit of TiO₂ catalyst for treating new MB samples.

Addition of TMAOH as a surfactant resulting in narrowing the band gap energy may be because of the interaction of interlaminar bonding between TiO₂ and TMAOH molecules. TMAOH being an organic alkaline when it reacts with Ti produces layers of tetramethylammonium titanate, and the layers were bonded by hydrogen bond. But TMAOH does not react entirely with Ti, thus indicating the presence of tetramethylammonium cations (TMA⁺) and OH[−] (Dong et al. 2010; Tan et al. 2015). Addition of TMAOH into the solution releases N–C (presence of amine group in TMAOH)

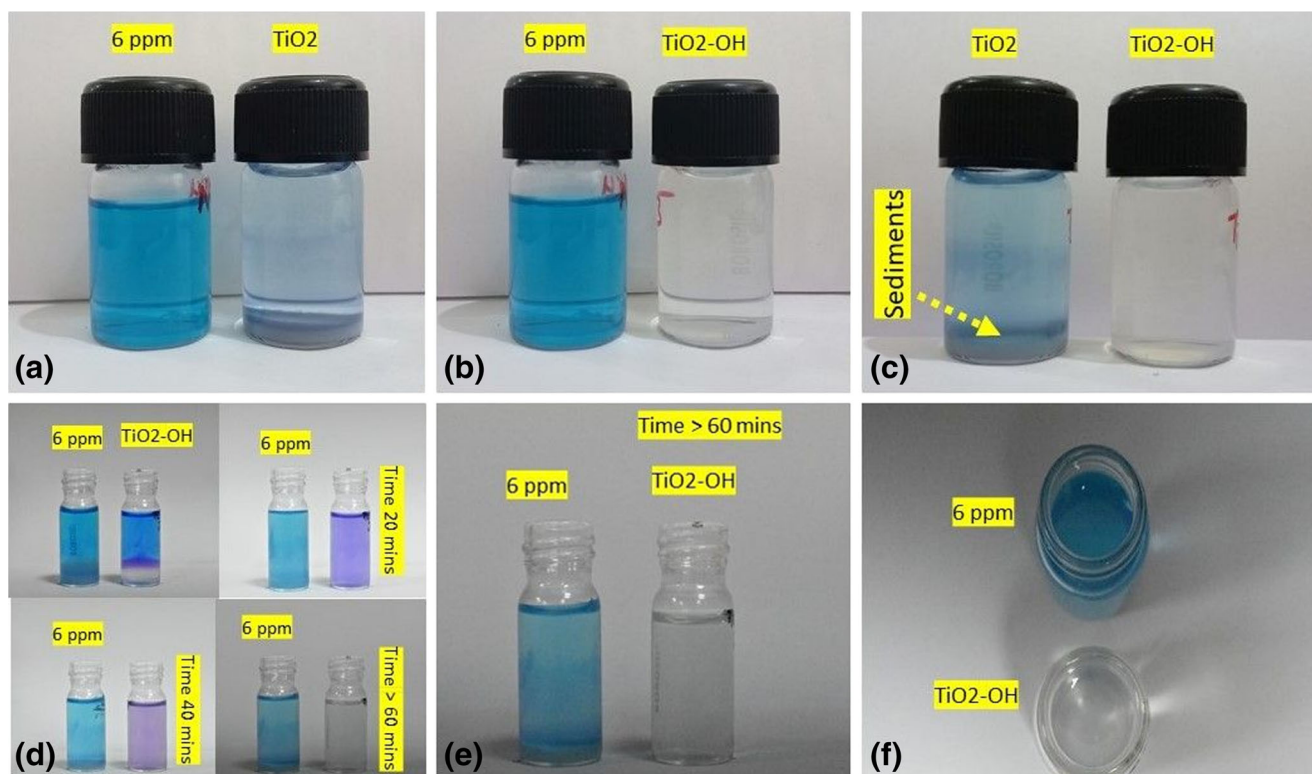


Fig. 2 Images of MB (6 ppm) raw sample and degradation process with **a** TiO₂ and **b** TiO₂-OH. **c** Sediments in TiO₂ and transparent solution in TiO₂-OH. **d** Stages of MB degradation using TiO₂-OH. **e** Comparison

with 6 ppm of raw sample shows transparency level after 60 min using TiO₂-OH and **f** aerial view of MB (6 ppm) and sample treated with TiO₂-OH

promising doping of non-metallic elements resulting in the enhancement of photocatalytic oxidation process. As N atom has strong electron affinity in TMA⁺ cations, it inhibits the recombination of e⁻/h⁺ by transfer of e⁻ from conduction band to TMA⁺ cations (Chen et al. 2007; Wang et al. 2020).

Adsorption of MB is more favorable in alkaline condition as it attains cationic configuration; availability of additional OH radicals leads to increase in the alkalinity of the solution by interfering in C⁻ S⁺ = C functional group and undergoing degrading oxidation of one (-CH₃) group. The presence of TMAOH with TiO₂ is responsible for the generation of OH radical scavenger as defined by Haber-Weiss reaction. OH radical is known to be one of the strongest and most important oxidizing agents. Along with TiO₂ and UV irradiation, OH radical is able to successfully initiate the complete oxidative mineralization of MB. Even though TMAOH is considered toxic to the environment if the range exceeds 30 mg L⁻¹, through the demethylation degradation, TMAOH can also be mineralized in the presence of UV irradiation on photocatalyst TiO₂. The degradation process of TMAOH involves the generation of OH radicals scavenger as explained by Haber-Weiss reaction; thus, generation of OH radical shows enhanced increase of MB degradation (Houasa et al. 2001; Diaz-Urbe et al. 2104; Huang et al. 2017; Cho et al. 2004; Nosaka and Nosaka 2016; Chiou et al. 2014).

The pH values are recorded for samples treated with TiO₂ and TiO₂-OH conditions. Three separate samples treated with TiO₂ and TiO₂-OH are tested to identify pH range. The average value in both samples is found to be 7.6 for TiO₂-treated samples and 7.8 for TiO₂-OH-treated samples. Due to the addition of TMAOH, the pH values increased to 8.5 during the photocatalytic reaction and reduced to 7.8 at the end of the reaction. As shown in Fig. 2, OH radicals break the bond of MB that is responsible for decolorization of the compounds (Wydra et al. 2015). MB has chromophore (N-S conjugated system on central aromatic heterocycle) and auxochrome (N-containing groups with a lone e⁻ pairs on benzene ring) groups, and these two compounds undergo the process of degradation during mineralization of MB resulting in decolorization (Yang et al. 2017). The decolorization process is dependent on the photocatalyst concentration, and lower availability of the photocatalyst with the ratio of dye concentration leads to reduced decolorization process. This process is visible in Fig. 2a as the photocatalytic treatment undertaken by using only TiO₂ with lesser concentration exhibits a mild trace of color. In the case of photocatalytic treatment using TiO₂ with additional OH groups, the decolorization is completely achieved. This confirms that even with a lower concentration of TiO₂ and with the enhancement of OH functional groups, the decolorization can be achieved at a faster rate.

Figure 2d shows the MB degradation process due to interaction with TiO₂-OH at different durations. The images indicate that the degradation process is initiated within 20 min and

the color of the solution is changed. At 60 min, the degradation is around 80% as shown in Fig. 1b from the photodegradation plot. This indicates the rapid transformation of the MB dye sample during reaction with the TiO₂-OH system. An aerial view of TiO₂-OH-treated samples and untreated samples is shown in Fig. 2f; this indicates the transparency level in the treated samples. In the case of the TiO₂ system, it took around 300 min to reach 80% degradation. This confirms that the degradation mechanism is rapid upon treatment with TiO₂-OH compared to TiO₂. The sedimentation of treated dye substance can be achieved only in the samples treated with TiO₂ systems compared to TiO₂-OH system.

Photodegradation efficiency and kinetics of sediments containing TiO₂

The sediment is used to treat new MB samples to validate the efficiency of reusing the TiO₂ samples. The sediment is used without any further treatment or drying process, and the analysis is carried out in new MB samples with the same 6 ppm concentration. A set of sediments isolated from the treated water is analyzed separately in two new MB samples. Samples consisting of TiO₂ along with sediments were taken separately to analyze the photocatalytic activity. Figure 3 shows the photodegradation efficiency profile, samples 1–3 represent the PDE of isolated sediments containing TiO₂ samples, and samples 4–6 represent sediments containing TiO₂ samples aged for 1 week. In both cases, the sediments are not dried or processed for treating new MB dye samples.

The absorbance spectra are measured after forward pipetting at each time interval for the given duration (20, 40, 60, 120, 180, 240, and 300 min). Sediments with new and

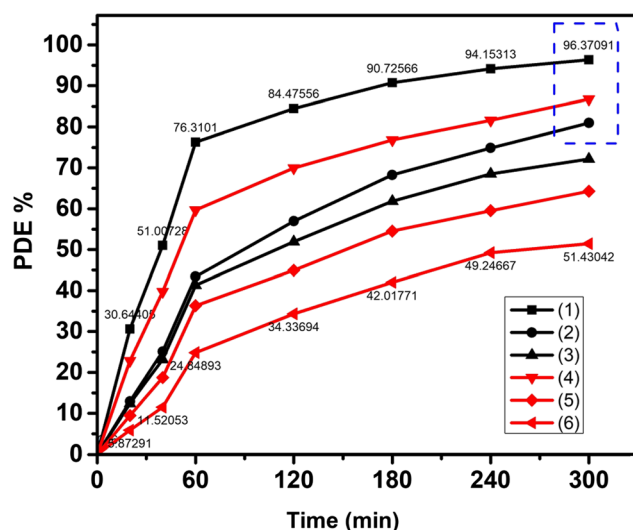


Fig. 3 PDE % of reusability of TiO₂ sediments (black line indicates reuse of fresh TiO₂ sediments instantaneously after degradation process, and red line indicates aged TiO₂ sediments reused after a week)

aged TiO₂ were able to react with new MB samples for three consecutive cycles. In Fig. 3, the label is mentioned for two samples which exhibit maximum and minimum PDE in the two categories of sediments. The freshly prepared TiO₂ nanoparticles show better PDE than aged sediments for this duration. TiO₂ gives 90% PDE in the first cycle of reuse, and the efficiency declines to 70% and 60% in further cycles of reuse. Efficiency of 80% is shown among the aged samples during the first cycle, and the efficiency reduced less than 60% after further cycles. A rectangular window indicated with dashed blue lines in Fig. 3 represents the samples which exhibit more than 70% PDE. The motive of this experiment is to analyze the reusability of sediments containing TiO₂ and to analyze the PDE on MB samples using new MB samples. This indicates that catalyst could show better PDE if it is reused at a shorter duration. This data proves that with the mentioned concentration of catalyst, it is possible to reuse the samples for treating fresh MB samples. This model can be scaled up to treat a large quantity of MB samples by reusing the sediments rather than preparing fresh TiO₂ nanoparticles.

Figure 4a shows pseudo-first-order kinetics for samples of sediments containing TiO₂ catalyst; Fig. 4b shows the kinetics of aged sediments containing TiO₂. Calculation of percentage removal of MB via adsorption is done by using $(C_0 - C_t / C_0)$ equation where C_0 and C_t are the concentrations of MB in solution at initial and final stages (Chen et al. 2015). The kinetics profile indicates that at the first cycles, the reaction rate is faster (0.0104 and 0.0061) compared to consecutive cycles in both samples. While comparing both samples, the reaction rate at cycle-2 shown in Fig. 4a is equivalent compared to cycle-1 shown in Fig. 4b; this indicates that aged samples exhibit less reaction rate with PDE less than 60% due to decreased stability and photocatalytic property of TiO₂ in the medium. At each interval, the supernatant is carefully separated for recording the absorbance and it is redispersed in the sample immediately after the measurements. This data gives precise information on the reusability of TiO₂ for photocatalytic activity along with reaction rate (Table 1).

Table 1 Comparison of MB dye degradation using TiO₂ nanoparticles reported in journals

% of dye degradation	Duration (min)	Reference
88.51	120	Wu and Huang (2010)
68	180	Yang et al. (2010)
91	720	Mukhlis et al. (2013)
92	120	Wei et al. (2013)
30	120	Wu and Tai (2013)
98	270	Chekir et al. (2016)
40	300	Nasikhudin et al. (2020)
85	300	Present study

FTIR and EDX of photocatalyst

FTIR and EDX analyses are performed for the treated water samples to identify the functional groups of the compounds and traces of elements, respectively. FTIR analysis is performed using conventional KBr pellet method. Figure 5a shows the FTIR plot consisting of two spectra of TiO₂ samples before and after the treatment. This spectrum is recorded to investigate the level of TiO₂ present in the sediments after the treatment. Similar spectra are recorded for the samples treated with TiO₂-OH conditions. Figure 5a shows two spectra indicated as TiO₂ and sediment with functional groups Ti–O–Ti (650 cm⁻¹), OH bending (1635 cm⁻¹ and 1636 cm⁻¹), and OH (3366 cm⁻¹ and 3326 cm⁻¹) stretching and sediment consisting the same functional groups in the reduced quantity. There is reduction of 45% in OH stretching regime, 27% in OH bending regime, and 51% in Ti–O–Ti regime. This ratio confirms that quantity of Ti–O–Ti is reduced into half in sediment during the final duration of the photocatalytic treatment. This is due to suspensions of unreacted photocatalyst molecules, and the peak at 1026 cm⁻¹ represents the aliphatic amine groups from methylene blue samples (Barisci et al. 2016). The sediments are clearly observed in Fig. 2c with

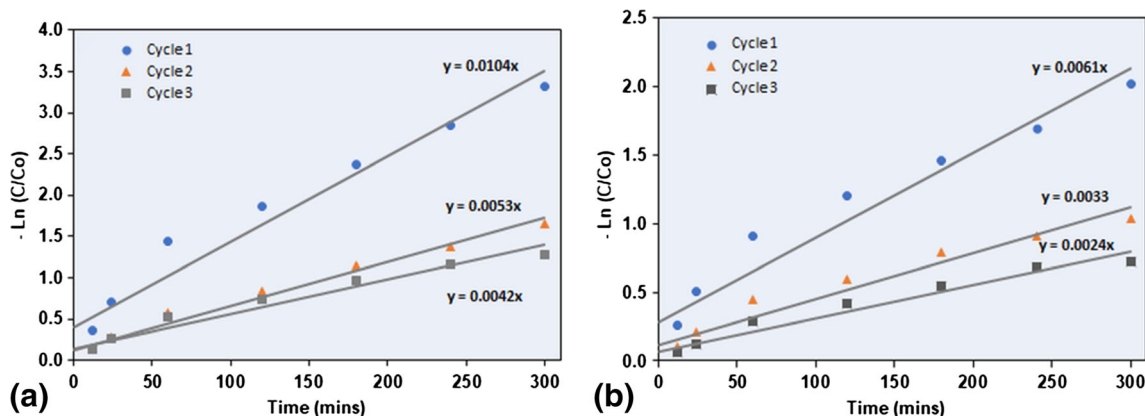


Fig. 4 Pseudo-first-order kinetics study on photodegradation of MB in multiple cycles. **a** TiO₂ sediments collected and analyzed instantly. **b** TiO₂ sediments reused after 1 week

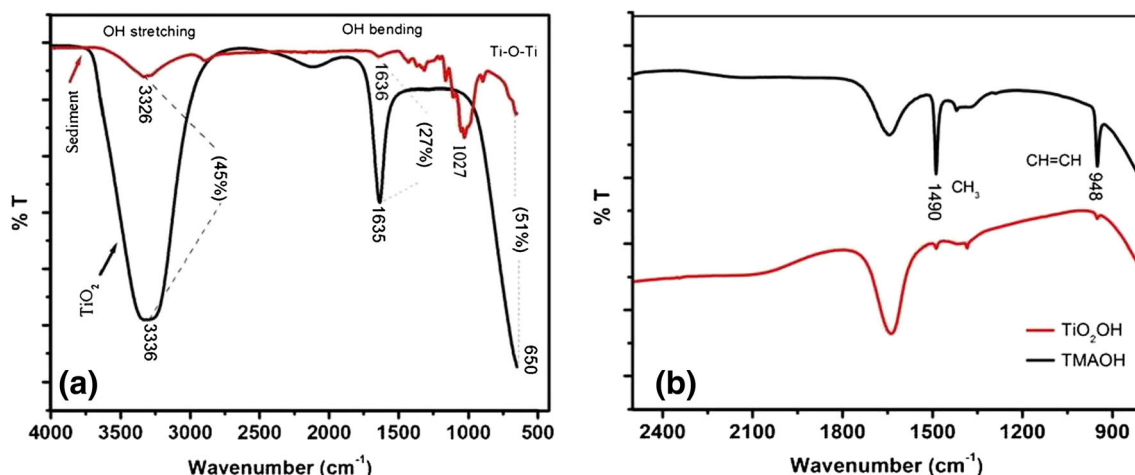


Fig. 5 FTIR plot of **a** TiO_2 before and after treatment (black line indicates TiO_2 samples to be used for degradation, and red line indicates the sediments). **b** Spectra of TMAOH and TiO_2 -TMAOH

bluish color traces. Apart from a peak at 1026 cm^{-1} , the sediments did not exhibit any peaks of other functional groups present in the methylene blue. Figure 5b shows comparative spectra of TiO_2 -OH and TMAOH; functional groups at 1490 cm^{-1} and 948 cm^{-1} indicate the TMAOH sample, and the same groups appear at TiO_2 -OH sample but the peak intensity is not predominant due to less quantity of TMAOH present in the TiO_2 -OH samples after the treatment process. EDX and CV analyses were performed exclusively to detect the traces of TiO_2 and TMAOH, respectively.

EDX measurements were performed to identify traces of elements after the treatment process. The supernatant is separated after the treatment process and allowed to dry under vacuum conditions. Figure 6a and b show the EDX plot for TiO_2 nanoparticles (sediments) and supernatant of the treated water. EDX plot indicates that there are no traces of TiO_2 in the supernatant after the treatment process. The traces of Ti and O are present in sediment after the treatment process. This shows that the sedimentation is initiated by reaction of particles with dye molecules and promotes flocculation. In case of samples treated by TiO_2 -OH, traces of Ti are not detectable due to degradation of the photocatalyst by TMAOH during

the process. This analysis confirms that the supernatant is free from Ti, and treated samples were further analyzed for seed germination process.

SEM analysis

SEM image of powder TiO_2 reveals agglomeration of nanoparticles with non-uniform size distribution as shown in Fig. 7a, whereas TiO_2 dispersed in TMAOH, liquid monodispersed nanoparticles can be identified at some extent which clearly indicates that addition of TMAOH as surfactant decreases the agglomeration of TiO_2 particles (Fig. 7b).

Water quality and CV measurements

The objective of this experiment is to analyze the quality of the treated water for seed germination. To validate this task, the samples are further subjected for water quality and CV analysis. Water quantity parameters are analyzed for the samples with dye-infiltrated water and treated water. Among these parameters, turbidity (NTU), calcium, magnesium, equivalent mineral acidity, phosphate, aluminum, and sulfate levels are

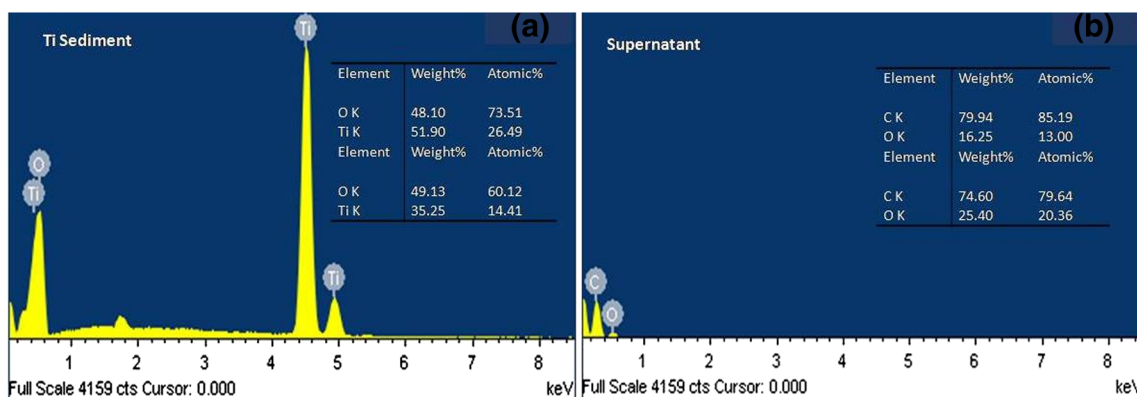


Fig. 6 EDX plot of **a** TiO_2 sediments examined after the degradation process. **b** After the treatment process, supernatant shows no traces of Ti

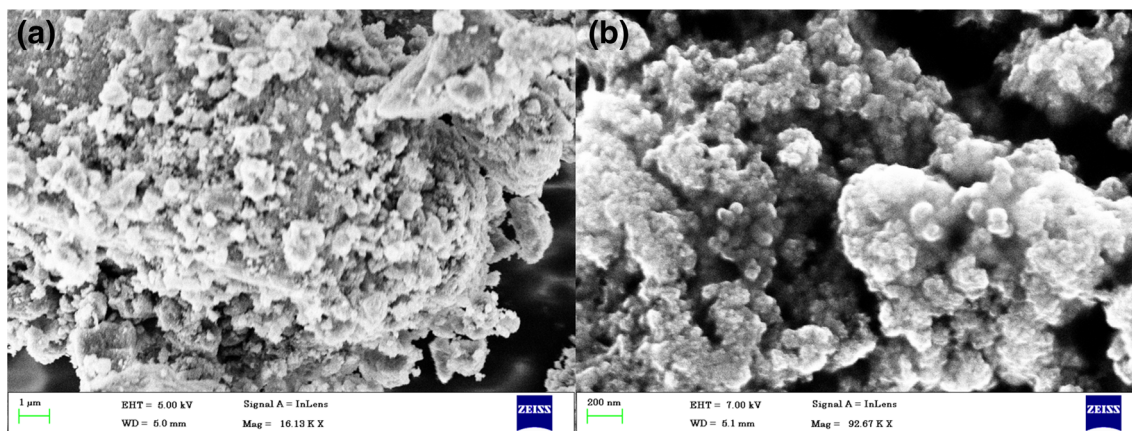


Fig. 7 Scanning electron micrograph (SEM) of **a** powder TiO_2 synthesis through hydrothermal process and **b** dispersion of powder TiO_2 into TMAOH

common in the range < 0.1 (mg L^{-1}). Conductivity, TDS, bicarbonate, and chloride levels are slightly higher in treated water compared to those in dye-infiltrated water. The conductivity values are 140 and 200 micromhos cm^{-1} ; TDS values are 108 and 130 mg L^{-1} ; chloride range is 14.7 and 20.3 mg L^{-1} for untreated and treated samples, respectively; and the range is under permissible limit. Total hardness, biochemical oxygen demand (BOD) (3 days), and chemical oxygen demand (COD) are low in treated water compared to those in untreated water. The range of total hardness is 9 and 6 mg L^{-1} , BOD values are 8 and 1.5 mg L^{-1} , and COD values are 40 and 13.4 mg L^{-1} for untreated and treated water samples. Among the parameters, BOD value decreased to 1.5 from 8 mg L^{-1} after the treatment process. BOD of natural waters like pristine rivers exhibit values below 1 mg L^{-1} , and severely polluted waters exceed the range of 8 mg L^{-1} as per the reports (Grover and Wats 2013). High COD value indicates an increased level of pollutants in the water and one of the important parameters in water quality analysis of wastewater treatment (Guoqing et al. 2011). Effect of TiO_2 photocatalyst for degradation of methylene blue and analysis of COD and BOD levels are reported (Sari et al. 2017). The experiments conducted in this work focus on the samples treated with $\text{TiO}_2\text{-OH}$ and their effect on COD and BOD. The reports show that the treated samples exhibit plausible BOD and COD range which is suitable for scale-up process in treatment plants for irrigation and plantation purposes.

CV of the TMAOH solution was performed on Screen-Printed Carbon Electrodes DropSens© 110 series using 3-electrode electrochemical system (Model CHI 660C) where two separate carbon electrodes act as working electrode and counter electrode, whereas silver/silver chloride electrode acts as reference electrode. CV of different concentrated TMAOH and trace solution was taken in the potential range of -0.2 to 0.8 V with respect to reference electrode at a scan rate of 5 mV S^{-1} . A certain amount of solution was dropcasted on the electrodes, and cyclic voltammetry was performed using CHI 660C interfaced with computer.

The permissible discharge limit for TMAOH is 30 mg L^{-1} since exceeding this limit is considered toxic for the environment and aquatic life (Chang et al. 2019). To identify the traces of TMAOH, the samples are analyzed using CV techniques with Screen-Printed Carbon Electrodes DropSens© 110 series. The CV plot of the different concentrated TMAOH solution (fM to μM) along with trace solution is shown in Fig. 8a. The figure shows that the redox peak is decreasing with decrease of the concentrations of TMAOH solution. Figure 8b shows the CV of the fM concentrated TMAOH and CV of trace solution. It is clearly observable that no peak of TMAOH is found from the treated solution compared to fM concentrated TMAOH solution. Hence, CV proves that the treated solution is free of TMAOH and it does not restrain the seed germination process.

Seed germination

Vigna radiata seeds were analyzed for the germination process with 1 ml of treated water samples and growth was observed for 6 days. Untreated water with 6 ppm MB is also used to observe the germination process. In both cases, the growth was observed; further length of root and shoot is measured. Root is the prominent point for uptaking minerals and nutrients present in the soil and water. Average root and shoot lengths observed for samples with Milli-Q water are 9.5 and 8.5 cm, water treated with TiO_2 is 5.75 and 5.5 cm, and water treated with $\text{TiO}_2\text{-OH}$ is 5.5 and 6 cm. The same analysis was performed using untreated samples of MB in concentrations 6 ppm, 20 ppm, and 40 ppm; the results show that root and shoot lengths are 6.5 and 9 cm, 5.5 and 7.25 cm, and 2.75 and 6.25 cm, respectively.

The profile confirms that the germination of seeds and growth phase is not inhibited by the presence of the effect of dyes for mentioned concentration as shown in Fig. 9. The growth rate of plants in untreated water consisting of MB clearly shows the absorption of MB exhibited by color traces on the plant as denoted in Fig. 9b. This indicates that the dye is

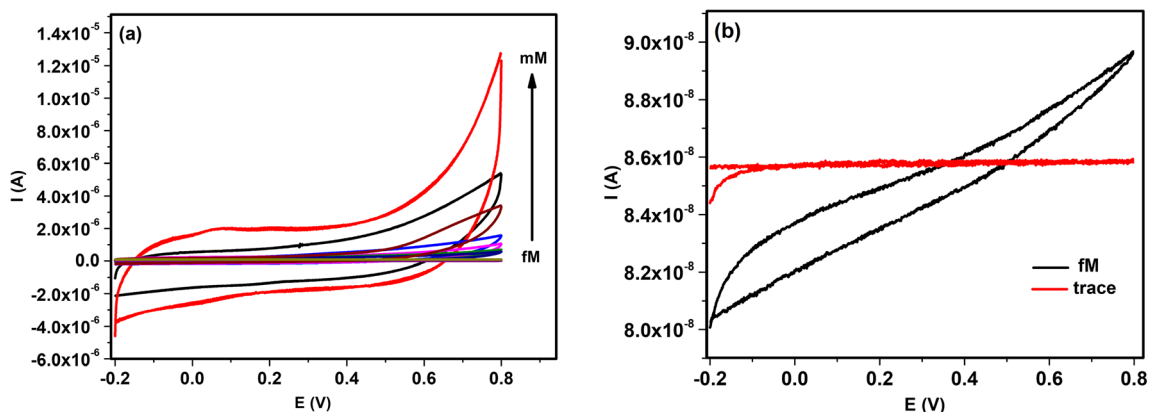


Fig. 8 CV plot of **a** different TMAOH concentrations (fM to μ M) from prepared aliquots. **b** Comparison of TMAOH with known (fM) concentration and TiO_2 -OH-treated samples to identify traces of TMAOH

absorbed by the plants through transpiration, but the growth of the plants was not inhibited as the concentration was low and time period of exposure was less but the transpiration rates in plants may be affected by the change in concentration and exposure period of MB. Even though plant growth was normal until a certain stage, due to the absorbance and retaining of dye molecules, the plant could not grow further due to hurdles created on pathway by dye molecules that will prevent absorption and mobilization of essential nutrients like proteins and carbohydrates that were stored in the germinating seeds (Sethy and Ghosh 2013; Yu et al. 2015). Further absorption of MB by the plants was confirmed by placing horizontal sections of plant shoot under a microscope as shown in Fig. 9c. Considering this factor, the treated water samples were analyzed to detect the trace elements of nanoparticles and other chemicals.

Distribution plot is shown in Fig. 10. The x-axis indicates root and shoot lengths from the proximal point; the negative numbers indicate the downwards direction of root growth from the proximal point. The in vitro hydroponics experiments are conducted by analyzing the seed germination and growth using treated water and MB infiltrated water. The germination process is performed in 10-ml glass vials as shown in Fig. 9 under the influence of natural environmental and

sunlight conditions. Although the germination process in wet soil can enhance the growth factor, the experiments are performed to analyze the uptake of treated and untreated water by seed for germination process. Figure 10a shows the distribution of root and shoot for samples of control (Milli-Q water) and treated water using TiO_2 and TiO_2 -OH, respectively. This plot indicates that the root and shoot distribution for control is more than that of samples with treated water. This indicates that water is absorbed and initiated the seed germination process. All the water samples (control, treated samples and MB infiltrated water) are added only once during the initial stage of the process. The root and shoot distribution of samples influenced by TiO_2 and TiO_2 -OH exhibits equal root and shoot lengths from the proximal point; this indicates the treated water acts neutral without any additional nutrients for enhancing the growth of the plant. The root-shoot ratio determines the ability of the plants to absorb nutrients in case of higher root proportion and absorb more light in case of more shoot proportion. The root-shoot predicts the favorable parameters for effective growth of the plants (Harris 1992). In the case of MB-infiltrated water, the root-shoot ratio increases with an increase in MB concentration (6, 20, and 40 ppm) as shown in Fig. 10b. This is due to the organic additives present in MB that enhance the growth of the plants. Although the

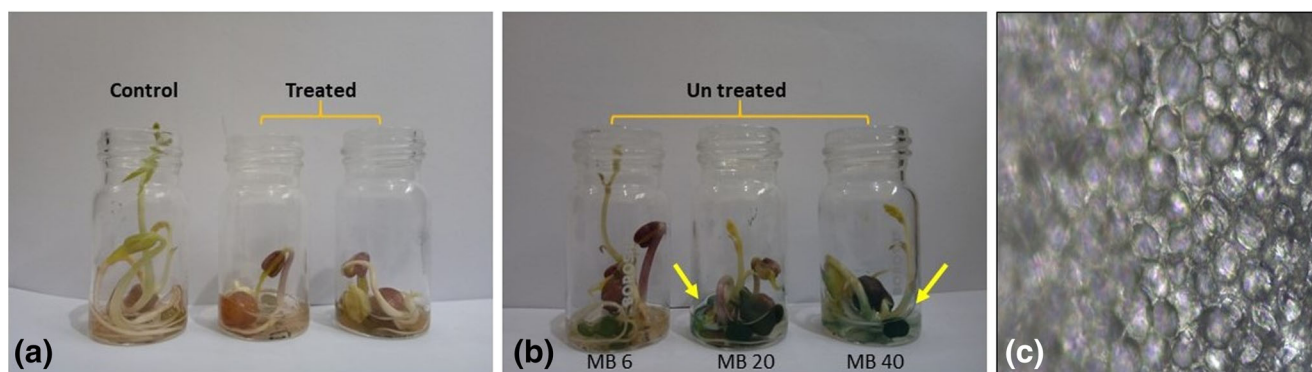


Fig. 9 Seed germination process using **a** Milli-Q water as control, treated water using TiO_2 and TiO_2 -OH. **b** Untreated water using MB-infiltrated water (6, 20, and 40 ppm). **c** Microscopic image of the cross section of stem shows traces of MB (6 ppm)

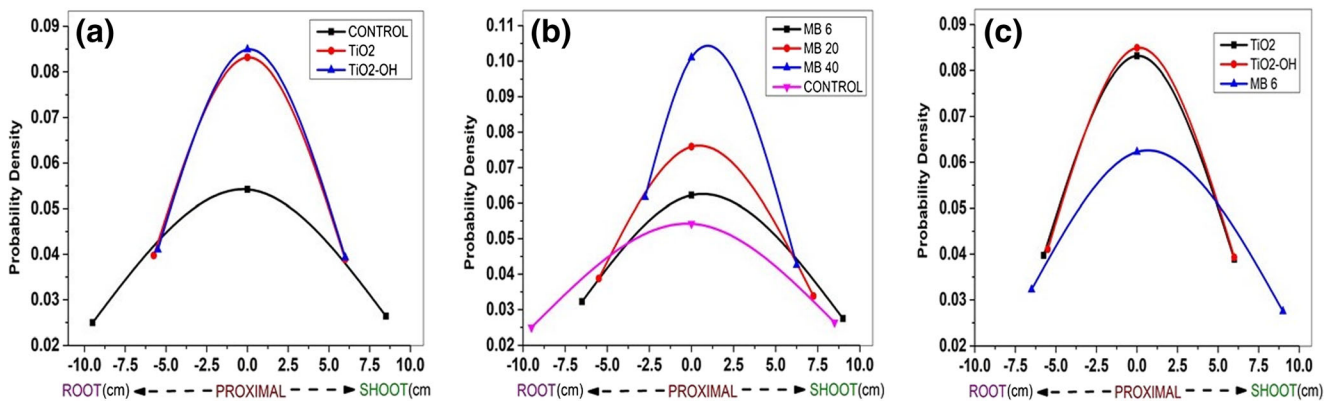


Fig. 10 Comparative distribution plot of root and shoot growth for **a** control, TiO₂, and TiO₂-OH. **b** MB (6, 20, 40 ppm) and control. **c** TiO₂, TiO₂-OH, and MB (6 ppm)

growth is supported by MB-infiltrated water, this leads to the decomposition of the plant due to immobilized dye traces in their system for a prolonged duration. Figure 10c shows the comparative plot of root and shoot distribution MB (6 ppm), TiO₂, and TiO₂-OH. The plot indicates that the root-shoot ratio is higher with MB (6 ppm) compared to that in treated water. The treated water exhibits identical root-shoot distribution from the proximal level, and this indicates that upon addition of more treated water, the root-shoot ratio will increase with the proper growth of the plant. This also confirms that the treated water can be reused for irrigation and plantation after post-processing techniques such as addition of minerals to the water. The treatment process can be scaled up to large quantities to reuse processed contaminated water for irrigation and plantation purposes. Considering the enormous quantity of water requirements for irrigation and plantation, dye degradation using TiO₂ and TiO₂-OH materials can be adapted to treat contaminated water. Although several processes are involved in treating the contaminated water and in reuse for irrigation and plantation, this simple and cost-effective technique can be utilized at the minimum to degrade the dye and reuse the water for irrigation and plantation purposes.

Conclusion

Photocatalytic degradation of methylene blue is demonstrated with TiO₂ and TiO₂-TMAOH with reuse of TiO₂ samples from treated water. The samples treated with TiO₂-TMAOH show enhanced degradation efficiency compared to TiO₂ due to complementary OH groups supplied by TMAOH. Data of FTIR, EDX, and CV analyses confirm the absence of dye functional groups and metal ion traces in treated water, respectively. Furthermore, water quality analysis showed an improved level of BOD for the treated water. Seed germination experiments using treated water show a growth response. The outcomes of the experiments show that the photocatalyst is

stable to treat dye-infiltrated water for three cycles to retain (70–90%) photodegradation efficiency. The treated water acts as a supportive platform for the seed germination process with the specified quantity of water. This study can be further extended to monitor the germination of other seed varieties and life cycle analysis. This result explores the new platform to analyze the treated water for reusability of photocatalyst and utilize the treated water for plantation and irrigation process.

Acknowledgements The author would like to thank the laboratory support of the Division of Environmental Science, Department of Water and Health, JSS Academy of Higher Education and Research, Mysuru and Optics and Microfluidics Instrumentation Lab, Department of Instrumentation and Applied Physics, Indian Institute of Science, Bengaluru.

Author contribution KS (PhD student) has sampled *Vigna radiata*, analyzed, and interpreted the results. SHP provided instrumentation and reagents in the laboratory. VSR performed the scientific work and was a major contributor in writing the manuscript. SSG provided instrumentation and reagents in the laboratory. All the authors read and approved the final manuscript.

Data availability All data generated or analyzed during this study are included in this published article.

Declarations

Consent to participate Not applicable

Consent for publication Not applicable

Competing interests The authors declare no competing interests.

References

Akpan UG, Hammed BH (2009) Parameters affecting photocatalytic degradation of dyes using TiO₂-based photocatalysts: a review. J

- Hazard Mater 170:520–529. <https://doi.org/10.1016/j.jhazmat.2009.05.039>
- Andrade AL, Fabris JD, Ardisson JD, Valente MA, Ferreira JMF (2012) Effect of tetramethylammonium hydroxide on nucleation, surface modification and growth of magnetic nanoparticles. *J Nanomater* 1:10. <https://doi.org/10.1155/2012/454759>
- Barışçi S, Turkyay O, Dimoglo A (2016) Review on grey water treatment and dye removal from aqueous solution by ferrate (VI). *ACS:350–409*. <https://doi.org/10.1021/bk-2016-1238.ch014>
- Chang DT, Park D, Zhu JJ, Fan HJ (2019) Assessment of an MnCe-GAC treatment process for tetramethylammonium-contaminated wastewater from optoelectronic industries. *Appl Sci* 9:4578. <https://doi.org/10.3390/app9214578>
- Chekir N, Benhabiles O, Tassalit D, Laoufi NA, Bentahar F (2016) Photocatalytic degradation of methylene blue in aqueous suspensions using TiO₂ and ZnO. *Desalin Water Treat* 57(13):6141–6147. <https://doi.org/10.1080/19443994.2015.1060533>
- Chen Y, He X, Zhao X, Yuan Q, Gu X (2007) Preparation, characterization, and growth mechanism of a novel aligned nanosquare anatase in large quantities in the presence of TMAOH. *J Colloid Interface Sci* 310(1):171–177. <https://doi.org/10.1016/j.jcis.2007.01.046>
- Chen CC, Hu SH, Fu YP (2015) Effects of surface hydroxyl group density on the photocatalytic activity of Fe³⁺-doped TiO₂. *J Alloys Compd.* 632:326–334. <https://doi.org/10.1016/j.jallcom.2015.01.206>
- Chiou CS, Chuang KJ, Lin Y-F, Chen HW, Ma CM (2014) Application of ozone related processes to mineralize tetramethylammonium hydroxide in aqueous solution. *Int J Photoenergy* 170:520–529. <https://doi.org/10.1016/j.jhazmat.2009.05.039>
- Cho M, Chung H, Choi W, Yoon J (2004) Linear correlation between inactivation of *E. coli* and OH radical concentration in TiO₂ photocatalytic disinfection. *Water Res* 38:1069–1077. <https://doi.org/10.1016/j.watres.2003.10.029>
- Comparelli R, Fanizza E, Curri ML, Cozzoli PD, Mascolo G, Passino R, Agostiana A (2005) Photocatalytic degradation of nAzo dyes by organic-capped anatase TiO₂ nanocrystals immobilized onto substrates. *Appl Catal B Environ* 55:81–91. <https://doi.org/10.1016/j.apcatb.2004.07.011>
- Diaz-Urbe C, Vallejo W, Ramos W (2014) Methylene blue photocatalytic mineralization under visible irradiation on TiO₂ thin films doped with chromium. *Appl Surf Sci* 319:121–127. <https://doi.org/10.1016/j.apsusc.2014.06.157>
- Dong X, Tao J, Li Y, Zhu H (2010) Oriented single crystalline TiO₂ nano-pillar arrays directly grown on titanium substrate in tetramethylammonium hydroxide solution. *Appl Surf Sci* 256:2532–2538. <https://doi.org/10.1016/j.apsusc.2009.10.100>
- Feizi H, Moghaddam PR, Shahtahmassebi N, Fotovat A (2012) Impact of bulk and nanosized titanium dioxide (TiO₂) on wheat seed germination and seedling growth. *Biol Trace Elem Res* 146(1):101–106. <https://doi.org/10.1007/s12011-011-9222-7>
- Grover AS, Wats M (2013) Decaying water bodies – victims of human neglect or urbanization. *IPCBE* 54: 48–52. <https://doi.org/10.7763/IPCBE>
- Guoqing W, Weihong B, Jiaming L, Guangwei F (2011) Determination of chemical oxygen demand in water using near-infrared transmission and UV absorbance method. *Chin Opt Lett* 31(6):1486–1489. [https://doi.org/10.3964/j.issn.1000-0593\(2011\)06-1486-04](https://doi.org/10.3964/j.issn.1000-0593(2011)06-1486-04)
- Gupta AK, Pal A, Sahoo C (2006) photocatalytic degradation of a mixture of crystal violet (basic violet 3) and methyl red dye in aqueous suspension using Ag⁺ doped TiO₂ Dyes Pigments. 69:224–232. <https://doi.org/10.1016/j.dyepig.2005.04.001>
- Harris RW (1992) Root-shoot ratios. *Arboric J* 18(1):39–42
- Houasa A, Lachheb H, Ksibi M, Elaloui E, Chantal G, Herrmann JM (2001) Photocatalytic degradation pathway of methylene blue in water. *Appl Catal B Environ.* 31:145–157. [https://doi.org/10.1016/S0926-3373\(00\)00276-9](https://doi.org/10.1016/S0926-3373(00)00276-9)
- Huang J, Wang KS, Liang C (2017) Oxidative degradation of tetramethylammonium hydroxide (TMAH) by UV/persulfate and associated acute toxicity assessment. *J. Environ. Sci. Health C* 0: 1–8. <https://doi.org/10.1080/10934529.2017.1318634>, 52.
- Khataee AR, Pons MN, Zahraa O (2009) Photocatalytic degradation of three azo dyes using immobilized TiO₂ nanoparticles on glass plates activated by UV light irradiation: influence of dye molecular structure. *J Hazard Mater* 168:451–457. <https://doi.org/10.1016/j.jhazmat.2009.02.052>
- Kim JH, Lee HI (2003) Effect of surface hydroxyl groups of pure TiO₂ and modified TiO₂ on the photocatalytic oxidation of aqueous cyanide. *J Chem Eng* 21(1):116–122
- Mukhlsh MB, Najnin F, Rahman MM, Uddin MJ (2013) Photocatalytic degradation of different dyes using TiO₂ with high surface area: a kinetic study. *J Sci Res* 5(2):301–314. <https://doi.org/10.3329/jsr.v5i1.11641>
- Nasikhudin D, Kusumaatmaja MA Triyana, K. (2020). Enhancing photocatalytic performance by sonication and surfactant addition on the synthesis process of PVA/TiO₂ nanofibers membranes by electrospinning method. In *AIP Conference Proceedings* (Vol. 2251, No. 1, p. 040045). AIP Publishing LLC. <https://doi.org/10.1063/5.0017654>
- Natarajan TS, Thomas M, Natarajan K, Bajaj HC, Tayade RJ (2011) Study on UV-LED/ TiO₂ process of degradation of Rhodamine B dye. *Chem Eng J* 169:126–134. <https://doi.org/10.1016/j.cej.2011.02.066>
- Neppolian B, Choi HC, Sakthivel S, Arabindoo B, Murugesan V (2002a) Solar light induced and TiO₂ assisted degradation of textile dye reactive blue 4. *Chemosphere* 46:1173–1181. [https://doi.org/10.1016/S0045-6535\(01\)00284-3](https://doi.org/10.1016/S0045-6535(01)00284-3)
- Neppolian B, Choi HC, Sakthivel S, Arabindoo B, Murugesan V (2002b) Solar light induced and TiO₂ assisted 561 degradation of textile dye reactive blue 4. *Chemosphere* 46:1173–1181. [https://doi.org/10.1016/S0045-25.5626535\(01\)00284-3](https://doi.org/10.1016/S0045-25.5626535(01)00284-3)
- Nosaka Y, Nosaka A (2016) Understanding hydroxyl radical (•OH) generation processes in photocatalysis. *ACS Energy Lett.* 1:356–359. <https://doi.org/10.1021/acsenergylett.6b00174>
- Rodriguez AAR, Montemayor SM, Porras CCL, Rodríguez FEL, Guerra EM, Domínguez MS (2017) CoFe₂O₄-TiO₂ hybrid nanomaterials: synthesis approaches based on the oil-in-water microemulsion reaction method. *J Nanomater.* 1, 15. <https://doi.org/10.1155/2017/2367856>
- Salehi M, Hashemipour H, Mirzaee M (2012) Experimental study of influencing factors and kinetics in catalytic removal of methylene blue with TiO₂ nanopowder. *American. J Environ Eng* 2(1):1–7. <https://doi.org/10.5923/j.ajee.20120201.01>
- Sari MI, Agustina TE, Melwita E, Aprianti T (2017, November) Color and COD degradation in photocatalytic process of procion red by using TiO₂ catalyst under solar irradiation. In *AIP Conference Proceedings* (Vol. 1903, No. 1, p. 040017). AIP Publishing LLC. <https://doi.org/10.1063/1.5011536>
- Sethy SK, Ghosh S (2013) Effect of heavy metals on germination of seeds. *J Nat Sc Biol Med* 4:272–275. <https://doi.org/10.1063/1.5011536>
- Smirnova N, Eremenko A, Fesenko T, Kosevich M, Snegir S (2019) UV–Vis spectroscopy and desorption/ionization mass spectrometry as the tools for investigation of adsorbed dye photodegradation. *Res Chem Intermediat* 45(8):4163–4177. <https://doi.org/10.1007/s11164-019-03898-x>
- Stylidi M, Kondarides DI, Verykios XE (2003) Pathways of solar light-induced photocatalytic degradation of azo dyes in aqueous TiO₂ suspensions. *Appl Catal B Environ.* 40:271–286. [https://doi.org/10.1016/S0926-3373\(02\)00163-7](https://doi.org/10.1016/S0926-3373(02)00163-7)
- Stylidi M, Kondarides DI, Verykios XE (2004) Visible light-induced photocatalytic degradation of Acid Orange 7 in aqueous TiO₂

- suspensions. *Appl Catal B Environ* 47:189–201. <https://doi.org/10.1016/j.apcatb.2003.09.014>
- Tan Z, Sato K, Ohara S (2015) Synthesis of layered nanostructured TiO₂ by hydrothermal method. *Adv Powder Technol* 26(1):296–302. <https://doi.org/10.1016/j.apt.2014.10.011>
- Teh CM, Mohamed AR (2011) Roles of titanium dioxide an ion-doped titanium dioxide on photocatalytic degradation of organic pollutants (phenolic compound and dyes) in aqueous solutions: a review. *J Alloys Compd* 509:1648–1660. <https://doi.org/10.1016/j.jallcom.2010.10.181>
- Vallejo W, Uribe CD, Cantillo A (2015) Methylene blue photocatalytic degradation under visible irradiation on TiO₂ thin film sensitized with Cu and Zn tetracarboxy-phthalocyanines. *J. Photochem. Photobiol. A: Chemistry* 299:80–86. <https://doi.org/10.1016/j.jphotochem.2014.11.009>
- Wang R, Ma X, Hao K, Song L, Liu T, Dai P et al (2020) Facile synthesis of C, N-TiO₂ nanorods via layered-TMAH interlaminar bonding interaction and their enhanced catalytic performance. *Mater Res Express* 7(2):025022
- Wei X, Zhu G, Fang J, Chen J (2013) Synthesis, characterization, and photocatalysis of well-dispersible phase-pure anatase TiO₂ nanoparticles. *International Journal of Photoenergy*, 2013. <https://doi.org/10.1155/2013/726872>
- Wu JC, Huang CW (2010) In situ DRIFTS study of photocatalytic CO₂ reduction under UV irradiation. *Front Chem Eng* 4(2):120–126
- Wu, Y. C., & Tai, Y. C. (2013). Effects of alcohol solvents on anatase TiO₂ nanocrystals prepared by microwave-assisted solvothermal method. *J Nanopart Res.*, 15(6): 1686.
- Wu CY, Tu KJ, Deng JP, Lo YS, Wu CH (2017) Markedly enhanced surface hydroxyl groups of TiO₂ nanoparticles with superior water-dispersibility for photocatalysis. *Materials* 10:566. <https://doi.org/10.3390/ma10050566>
- Wydra RJ, Oliver CE, Anderson KW, Dziubla TD, Hilt JZ (2015) Accelerated generation of free radicals by iron oxide nanoparticles in the presence of an alternating magnetic field. *RSC Adv* 5(24): 18888–18893. <https://doi.org/10.1039/C4RA13564D>
- Yang J, Peterlik H, Lomoschitz M, Schubert U (2010) Preparation of mesoporous titania by surfactant-assisted sol–gel processing of acetaldoxime-modified titanium alkoxides. *J Non-Cryst Solids* 356(25–27):1217–1227. <https://doi.org/10.1016/j.jnoncrysol.2010.04.035>
- Yang C, Dong W, Cui G, Zhao Y, Shi X, Xia X, Tang B, Wang W (2017) RSC Adv 7: 23699–23708. <https://doi.org/10.1039/c7ra02423a>, Highly efficient photocatalytic degradation of methylene blue by P2ABSA-modified TiO₂nanocomposite due to the photosensitization synergetic effect of TiO₂and P2ABeSA.
- Yu XZ, Feng YX, Yue DM (2015) Phytotoxicity of methylene blue to rice seedlings. *Global J Environ Sci Manage.* 1(3):199–204
- Yuan H, Ma S, Wang X, Long H, Zhao X, Yang D, Lo WH, Tsang YH (2019) RSC Adv 9: 5891–5894. <https://doi.org/10.1039/c8ra10172h>, Ultra-high adsorption of cationic methylene blue on two dimensional titanate nanosheets.
- Zhang H, Zhang W, Zhao M, Yang P, Zhu Z (2017) A site-holding effect of TiO₂ surface hydroxyl in the photocatalytic direct synthesis of 1, 1-diethoxyethane from ethanol. *Chem Commun* 53:1518–1521. <https://doi.org/10.1039/c6cc09050h>
- Zhao J, Wu T, Wu K, Oikawa K, Hidaka H, Serpone N (1998) Photoassisted degradation of dye pollutants. 3. Degradation of the cationic dye Rhodamine B in aqueous anionic surfactant/TiO₂ dispersions under visible light irradiation: evidence for the need of substrate adsorption on TiO₂ particles. *Environ Sci Technol.* 32: 2394–2400. <https://doi.org/10.1021/es9707926>

Publisher's note Springer Nature remains neutral with regard to jurisdictional claims in published maps and institutional affiliations.